

An Investigation of the Role of Cross-Linking and Photodegradation of Side-Chain Coumarin Polymers in the Photoalignment of Liquid Crystals

Peregrine Orr Jackson and Mary O'Neill*

Department of Physics, The University of Hull, Hull, HU6 7RX U.K.

Warren Lee Duffy, Paul Hindmarsh, Stephen Malcom Kelly, and Gareth James Owen

Department of Chemistry, The University of Hull, Hull, HU6 7RX U.K.

Received July 24, 2000. Revised Manuscript Received October 31, 2000

A surface anisotropy has been shown previously to be induced in thin films of photoreactive coumarin side-chain polymers by polarized UV illumination. Consequently, the resultant cross-linked polymer layers can be used as photoalignment layers for liquid crystal displays. Homogeneous alignment of a nematic liquid crystal in contact with a layer of a model coumarin side chain polymer is obtained with the director parallel or perpendicular to the UV polarization axis depending on the incident fluence. Spectroscopic analysis of the alignment layer now confirms that both photodegradation and cross-linking occur with different dependencies on fluence. Low UV fluences give parallel photoalignment and high cross-linking reactivity. However, the residual, unreacted polymer side chains show negligible anisotropy because of their freedom to move in an isotropic fashion. Hence, parallel liquid crystal alignment is attributed to a steric interaction between the liquid crystal and syndimerized side chains of the cross-linked polymer. A switch of the photoalignment direction accompanies the subsequent development of anisotropy of the intact, unreacted polymer side chains. The side-chain anisotropy and hence perpendicular liquid crystal alignment is ascribed to photodegradation rather than cross-linking.

Introduction

There is widespread interest in the development of alternative alignment technologies to rubbed polyimide for liquid crystals displays (LCDs) using nematic liquid crystalline mixtures. Particular attention is being paid to photoalignment techniques that involve the photochemical generation of a surface anisotropy in an alignment film and the subsequent macroscopic orientation of the liquid crystal (LC) director at the surface along the easy axis of the alignment layer in a stable and reproducible fashion. Photoalignment techniques would eliminate the need for mechanical buffing of the LCD substrate, which can result in pixel damage, static, and dust, and at the same time also allow subpixelated LCDs with improved viewing angle characteristics to be produced. The first reported example of photoinduced alignment was the illumination of a surface monolayer of azobenzene with unpolarized light to change the alignment of the adjacent nematic liquid crystal from homogeneous to homeotropic.¹ Polarized UV exposure was then found to induce an in-plane anisotropy to an azo-doped polymer and a preferred azimuthal orientation to the overlying nematic liquid crystal.² Reports of photoinduced LC alignment using other materials, such

as poly(vinyl cinnamate) (PVCi)³ and polyimide,⁴ and different alignment mechanisms, such as photochemical cross-linking and ablation, quickly followed. In a relatively short space of time photoalignment has become an important topic of research in the area of liquid crystals and LCDs.^{5–7} Although photoalignment of smectic liquid crystals has been demonstrated, the vast bulk of research in this area has been concerned with the alignment of the nematic phase, since almost all commercial LCDs utilize nematic liquid crystalline mixtures to generate their electrooptic effect. The physical causes of the macroscopic alignment of the director of a nematic liquid crystal by a photoalignment layer are the subject of some dispute. For example, the cinnamate polymer PVCi forms chemical cross-links on illumination with UV light via a (2 + 2) cycloaddition to form a cyclobutane dimer from two cinnamate groups and was first developed for use as a negative photoresist using isotropic UV light.⁸ However, it was found that when thin films of PVCi were illuminated with plane polarized UV light, the resultant cross-linked polymer

(1) Ichimura, K.; Suzuki Y.; Seki T.; Hosoki A.; Aoki K. *Langmuir* **1988**, *4*, 1214.

(2) Gibbons, W. M.; Shannon, P. J.; Sun S. T.; Swetlin B. J. *Nature* **1991**, *351*, 49.

(3) Dyadyusha, A.; Kozinkov, V.; Marusii, T.; Reznikov, Y.; Reshetnyak, V. Khizhnyak, A. *Ukr. Fiz. Zh.* **1991**, *36*, 1059.

(4) Hasegawa, M.; Taira, Y. *J. Photopolym. Sci. Technol.* **1995**, *8*, 241.

(5) Schadt, M. *Annu. Rev. Mater. Sci.* **1997**, *27*, 305.

(6) Ichimura, K. *Chem. Rev.* **2000**, *100*, 1847.

(7) O'Neill, M.; Kelly, S. M. *J. Phys. D: Appl. Phys.* **2000**, *33*, R67.

(8) Egerton, P.; Pitts, L. E.; Reiser, A. *Macromolecule* **1981**, *14*, 95.

network induced homogeneous liquid crystal alignment with the nematic director perpendicular to the polarization direction, \mathbf{P} , of the UV radiation.^{3,9} Alignment is thought to involve a dispersive LC–surface interaction and results from the anisotropic depletion of the cinnamate polymer side chains as a consequence of the (2 + 2) cycloaddition reaction.⁹ The photoproducts have an isotropic distribution so the anisotropy is postulated to originate from the intact polymer side chains, which have not yet reacted.^{3,10} Other authors suggest that the isomerization of the carbon–carbon double bond (C=C) of the cinnamate group from the trans isomer to the cis isomer is responsible for the alignment, especially at small fluences.^{11,12} However, the additional, potentially very important, effect of anisotropic photodegradation on the development of an azimuthal easy axis has not been considered in any detail. Although perpendicular alignment is mostly formed with PVCi type polymer layers, some structures give an azimuthal anchoring parallel to \mathbf{P} . Others show a switch in homogeneous alignment direction from parallel to perpendicular to \mathbf{P} depending on the irradiation conditions.^{13,14}

Unfortunately the poor thermal stability of photoalignment layers based on UV-irradiated PVC and its derivatives has so far prohibited their commercial exploitation in LCDs. Therefore, interest has switched to other classes of materials with an inert polymer backbone, such as acrylates, methacrylates, or polyvinyls, with new photoreactive side chains attached to the polymer, for potential use as photoalignment layers. Coumarin side-chain polymers invented and developed at ROLIC,^{15–17} such as those **1–6** shown in Table 1, which also cross-link by a (2 + 2) cycloaddition reaction on illumination with UV light, appear to possess the most promising photoalignment characteristics at the moment. The polymers **1** and **2** are discussed here in detail to illustrate their general behavior. The alignment obtained using these coumarin side chain polymers is chemically, electrochemically, photochemically, and thermally stable even after 100 hours at 120 °C.¹⁵ Highly photosensitive polymers have been developed, which provide strong anchoring: 24 mJ cm⁻² of polarized UV at 300 nm onto the polymer derivative **1** with a side chain formed from 6-hydroxycoumarin, see Figure 1, gives LC photoalignment with an azimuthal anchoring energy $>6 \times 10^{-5}$ J m⁻².¹⁰ Pretilt angles up to 7.5° have also been obtained using this polymer. Even higher pretilt angles using other coumarin derivatives have been reported.^{15–17} Figure 1 shows the structure of a typical coumarin side-chain polymer **1**, in this case a derivative of 6-hydroxycoumarin, and the head-to-head and head-to-tail cyclobu-

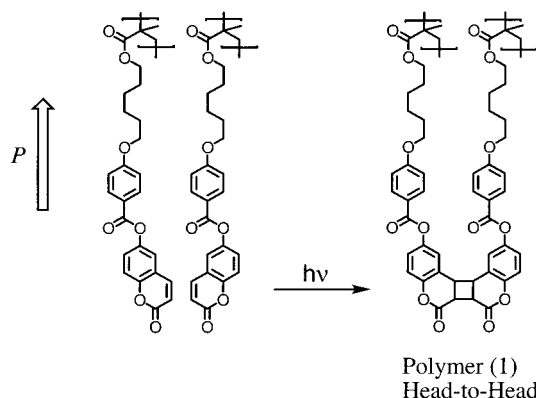


Figure 1. Chemical structure of **1** and its head-to-head dimer formed by (2 + 2) cycloaddition.

Table 1. Chemical Structure of the Photoreactive Coumarin Polymers (1–6)¹⁵ and Direction of Induced Alignment of the Easy Axis in the Azimuthal Plane with Respect to the Plane of Polarization of Incident UV

Molecular Structure	Low Fluence	High Fluence	ref
(1)	parallel	perpendicular	10
(2)	parallel	perpendicular	10,16
(3)	parallel	perpendicular	10,16,18
(4)	parallel	parallel	18
(5)	parallel	perpendicular	
(6)	parallel	parallel	16,18

tane dimers formed by irradiation with polarized UV light. There is also the possibility of the formation of *syn*- and *anti*-cyclobutane photoproducts. However, it is clear that cis/trans isomerization of the carbon–carbon double bond (in conjugation with the lactate carboxy function within the coumarin ring), which occurs in cinnamates, is not possible for coumarins. Schadt et al. report that the azimuthal alignment direction of side chain polymers containing derivatives of 7-hydroxycoumarin (umbelliferone), such as the polymethacrylate **2**, is parallel to the \mathbf{P} .¹⁷ Later work shows that for some structures the azimuthal LC alignment switches from parallel to perpendicular at a critical UV fluence.^{10,18,19} Molecular modeling and polarized FTIR

(9) Schadt, M.; Schmitt, K.; Kozinkov, V.; Chigrinov, V. G. *Jpn. J. Appl. Phys.* **1992**, *31*, 2135.

(10) Jackson, P. O.; Karapinar, R.; O'Neill, M.; Hindmarsh, P.; Owen, G. J.; Kelly, S. M. *Proc. SPIE* **1999**, *3635*, 38.

(11) Ichimura, K.; Akita, Y.; Akiyama, H.; Kudo, K.; Hayashi, Y. *Macromolecules* **1997**, *30*, 903.

(12) Tomita, H.; Kudo, K.; Ichimura, K. *Liq. Cryst.* **1996**, *20*, 171.

(13) Obi, M.; Morino, S.; Ichimura, K. *Jpn. J. Appl. Phys.* **1999**, *38*, L145.

(14) Kawatsuki, N.; Ono, H.; Takatsuka, H.; Yamamoto, T.; Sangen, O. *Macromolecules* **1997**, *30*, 6680.

(15) Schadt, M.; Seiberle, H. *J. SID* **1997**, *5/4*, 367.

(16) Herr, R.-P.; Herzog, F.; Schuster, A. Pat. Appl. WO 96/10049, 1996.

(17) Schadt, M.; Seiberle, H.; Schuster, A. *Nature* **1996**, *351*, 212.

(18) Obi, M.; Morino, S.; Ichimura, K. *Chem. Mater.* **1999**, *11*, 656.

(19) Hindmarsh, P.; Jackson, P. O.; Owen, G. J.; Kelly, S. M.; O'Neill, M.; Karapinar, R. *Mol. Cryst. Liq. Cryst.* **1999**, *332*, 439.

confirm that the polarization axis of cross-linked photoproducts is parallel to that of the incident UV.^{19,20} Hence, interactions between the LC and the photoproducts determine the alignment direction for short exposures, whereas above the critical fluence the alignment appears to be governed by the interaction with the unreacted polymer side chains. These have the lowest reactivity and, hence, maximum residual density perpendicular to **P**. The dispersive LC–coumarin interaction is larger than that of the LC–photoproduct because of the unbroken conjugation before dimerization of the side chains. This work aims to explain the surprising result that the latter determines the nematic director orientation at low fluences. Spectroscopic data will be used to elucidate the different origins of parallel and perpendicular alignment and why the resultant alignment direction should change at a critical fluence.

Experimental Section

LC Cell Preparation and Azimuthal Anchoring Energy Measurements. Thin films of the polymers were prepared by spin-casting solutions of the polymer in cyclopentanone onto clean InSnO-coated glass slides. The slides were subsequently baked at 90 °C in a nitrogen atmosphere. They were irradiated at room temperature using linearly polarized light of wavelength 300.5 nm from an argon ion laser. A constant incident power of 12 mW cm⁻² was used, and different spots were exposed with different fluences by changing the time for exposure. Commercial polyimide films (Nissan SE130) on InSnO-coated glass slides were prepared by spin casting followed by baking at 180° for 30 min. Hybrid 90° twisted-nematic (TN) cells of thickness ≈17 μm were constructed using one exposed alignment surface and one rubbed polyimide layer with perpendicular alignment directions. They were filled with E7 in its isotropic state to avoid creating flow alignment. In these devices, the actual twist angle, φ, may be less than the constructed twist angle, because of competition between surface and bulk forces. The cells were mounted on a polarizing microscope with the input polarizer arranged parallel to the rubbed direction. φ was found by rotating the analyzer to achieve maximum extinction. Assuming infinite anchoring at the rubbed polyimide surface, the azimuthal anchoring energy can be found from the equation

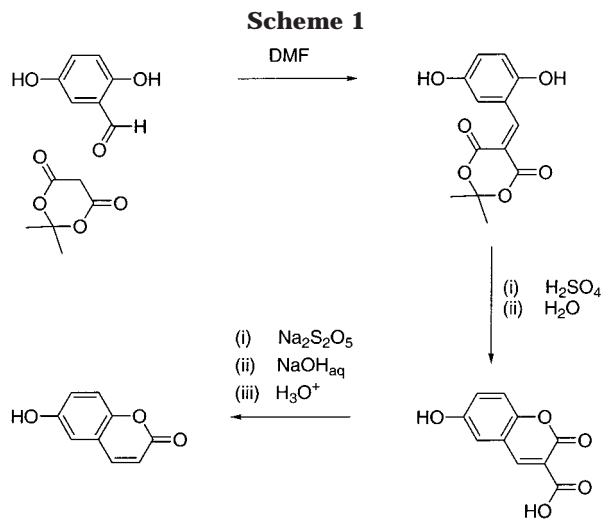
$$W_\phi = \frac{2K_{22}\phi}{\Lambda \sin 2\phi} \quad (1)$$

where K_{22} is the twist elastic constant and d the cell spacing measured before filling using a spectrophotometer. Φ , the angle between the LC alignment direction at the photoaligned surface and the polarization direction of the incident beam, is equal to ϕ or $90^\circ - \phi$ depending on whether the rubbing direction of the TN cell is parallel or perpendicular to **P**.

Birefringence Measurements. The birefringence of polymer **2** was measured during polarized UV illumination using a He Ne laser of wavelength $\lambda = 632.8$ nm as a probe beam. A sample of thickness $d = 300$ nm was deposited by spin casting onto a quartz slide and placed between crossed polarizers oriented at $\pm 45^\circ$ with respect to **P**. The transmitted intensity, I , of the probe beam through the system is given by

$$I = I_0 \sin^2\left(\frac{\pi \Delta n d}{\lambda}\right) \quad (2)$$

where Δn is the birefringence and I_0 is the transmitted intensity through parallel polarizers and an unexposed sample.



FTIR Measurements. The polymer was spin cast onto a CaF₂ substrate using standard procedures. FTIR measurements were carried out using a Perkin-Elmer Paragon 1000 spectrometer in the transmission mode. The absorbance spectra were measured before UV irradiation, and a sequence of exposures followed by FTIR measurements was made to monitor changes in the various absorption peaks with fluence.

Materials. 6-Hydroxycoumarin was synthesized as shown in reaction Scheme 1. The polymethacrylates **1** and **2** with a side chain incorporating 6-hydroxycoumarin and 7-hydroxycoumarin,¹⁶ respectively, were synthesized as depicted in reaction Scheme 2. The methods of preparation of the related polymethacrylate derivatives **3–5** of 7-hydroxycoumarin^{16,18} are shown in reaction Scheme 3. 4-Hydroxybenzoic acid, methacrylic acid, 6-bromo-1-hexanol, 6-bromohexanoic acid, 7-hydroxycoumarin, isopropylidene malonate (Meldrum's acid²¹), and 2,5-dihydroxybenzaldehyde were purchased from Aldrich and used as received. Reagent grade solvents were dried and purified as follows. *N,N*-Dimethylformamide (DMF) was dried over anhydrous P₂O₅ and purified by distillation. Butanone and methanol were distilled and stored over 5 Å molecular sieves. Triethylamine was distilled over potassium hydroxide pellets and then stored over 5 Å molecular sieves. Dichloromethane was dried by distillation over phosphorus pentoxide and then stored over 5 Å molecular sieves. Chloroform was alumina-filtered to remove any residual ethanol and then stored over 5 Å molecular sieves. ¹H nuclear magnetic resonance (NMR) spectra were obtained using a JEOL JMN-GX270 FT nuclear resonance spectrometer. Infrared (IR) spectra were recorded using a Perkin-Elmer 783 infrared spectrophotometer. Mass spectral data were obtained using a Finnegan MAT 1020 automated GC/MS. The purity of the reaction intermediates was checked using a CHROMPACK CP 9001 capillary gas chromatograph fitted with a 10 m CP-SIL 5CB capillary column. The purity of the final products was determined by high-performance liquid chromatography (HPLC) (5 μm, 25 cm × 0.46 cm, ODS Microsorb column, methanol, >99%) and by gel-permeation chromatography (GPC) (5 μm, 30 cm × 0.75 cm, 2 × mixed DPL columns, calibrated using polystyrene standards (molecular weights = 1000–4 305 000), toluene; no monomer present). The polymers were found to exhibit moderate to high M_w values (10 000–30 000) and acceptable M_w/M_n values (1.5–3). Melting points were determined using an Olympus BH-2 polarizing light microscope together with a Mettler FP52 heating stage and a Mettler FP5 temperature control unit. The thermal analysis of the polymers was carried out by a Perkin-Elmer DSC7-PC differential scanning calorimeter.

4-((6-Hydroxyhexyl)oxy)benzoic Acid. A solution of sodium hydroxide (4.4 g, 0.11 mol) and water (20 cm³) was

(20) Perny, S.; Le Barny P.; Delaire, J.; Buffeteau, T.; Sourisseau, C.; Dozov, I.; Forget, S.; Martinot Lagarde, P. *Liq. Cryst.* **2000**, *27*, 329.

(21) Armstrong, V.; Soto, O.; Valderrama, J. A.; Tapia, R. *Synth. Commun.* **1988**, *18*, 717.

washed with water (50 cm³), and then dried (Na₂SO₄). The filtered solution was evaporated down under reduced pressure, and the solid residue recrystallized from methanol to yield the desired acid (5.61 g, yield 61%), with Cr-SmA = 81 °C, SmC-SmA = 71 °C, SmA-N = 86 °C, and N-I = 97 °C (lit. mp 83 °C).¹⁶

¹H NMR (CDCl₃): δ 1.5 (m, 6H), 1.7 (quintet, 2H), 2.0 (s, 3H), 4.0 (t, 2H), 4.2 (t, 2H), 5.5 (quintet, 1H), 6.1 (m, 1H), 6.9 (d, 2H), 8.0 (d, 2H). IR (KBr pellet, cm⁻¹): 2960, 1720, 1690, 1610, 1430, 1320, 1260, 1170, 990, 850, 770, 650. MS (*m/e*): 306, 288, 260, 206, 138, 121, 83, 69, 55, 43.

5-(2,5-Dihydroxybenzylidene)-2,2-dimethyl-1,3-dioxinane-4,6-dione. Isopropylidene malonate (1.44 g, 0.01 mol) was added dropwise to a stirred solution of 2,5-dihydroxybenzaldehyde (1.38 g, 0.01 mol) in *N,N*-dimethylformamide (15 cm³). After being stirred for 30 min, the reaction mixture was left to stand for 12 h at room temperature. The resultant precipitate was filtered off and washed with cold water (3 × 10 cm³). The product was then recrystallized from a 3:1 mixture of ethanol and water to yield greenish yellow crystals (1.90 g, yield 72.0%), which were used in the next step without further purification.

6-Hydroxy-2-oxo-2H-1-benzopyran-3-carboxylic Acid. 5-(2,5-Dihydroxybenzylidene)-2,2-dimethyl-1,3-dioxinane-4,6-dione (1.90 g, 7.1 mmol) was added in portions to a stirred solution of concentrated sulfuric acid at 0 °C. The resultant reaction mixture was allowed to warm to room temperature over 2 h, poured onto crushed ice, and left overnight. The resultant precipitate was filtered off, pressed dry, and then recrystallized from a 2:1 mixture of acetone and water to give the desired acid (1.05 g, yield 71.0%), mp 294–296 °C.

¹H NMR (CDCl₃): δ 7.12–7.16 (d, 1H), 7.2 (d, 1H), 7.25 (d, 1H), 8.5 (s, 1H), 10.0 (s, 1H), 13.0 (s, 1H). IR (KBr pellet, cm⁻¹): 3200, 1740, 1710, 1680, 1560, 1310, 825. MS (*m/e*): 206 (M⁺), 162, 134, 105, 78, 63, 51, 45.

6-Hydroxycoumarin. A solution of 6-hydroxy-2-oxo-2H-1-benzopyran-3-carboxylic acid (0.84 g, 4.1 mmol) and 20% aqueous sodium metabisulfite solution was warmed at 60 °C with a lime water bubbler. When the evolution of CO₂ had stopped, the solution was heated under reflux for 30 s and then 50% aqueous potassium hydroxide solution (45 cm³) was added in a steady stream to the boiling solution. After completion of the addition the red solution was boiled for a further 10 s and then rapidly cooled to -78 °C. Concentrated hydrochloric acid (60 cm³) was added dropwise at -78 °C and the resultant solution kept at this temperature for 2 h. The resultant precipitate was then filtered off, washed with cold water (2 × 25 cm³), pressed dry, and then recrystallized from a 5:1 mixture of acetone and water to give the desired phenol (0.41 g, yield 68.3%), mp 249–252 °C (lit. mp 248–250 °C).²²

¹H NMR (CDCl₃): δ 6.35 (d, 1H), 6.95 (d, 1H), 7.05 (d, 1H), 7.15 (d, 1H), 7.7 (d, 1H), 9.25 (s, 1H). ¹³C NMR (CDCl₃/DMSO): δ 160.6, 153.4, 143.0, 119.6, 118.7, 116.7, 115.9, 111.9. IR (KBr pellet, cm⁻¹): 3200, 1740, 1680, 1560, 1310, 825. MS (*m/e*): 162 (M⁺), 134, 105, 78, 63, 51.

6-[(4-((6-(Methacryloyloxy)hexyl)oxy)benzoyl)oxy]coumarin. A solution of *N,N*-dicyclohexylcarbodiimide (0.34 g, 0.0017 mol) and dichloromethane (25 cm³) was added dropwise to a stirred solution of 6-hydroxycoumarin (0.27 g, 0.0017 mol), 4-((6-(methacryloyloxy)hexyl)oxy)benzoic acid (0.51 g, 0.0017 mol), 4-(dimethylamino)pyridine (0.20 g, 0.0017 mol), and dichloromethane (25 cm³) at 0 °C. The solution was then filtered and the solvent removed under reduced pressure. The residue was the purified using column chromatography on silica gel (5% ethyl acetate in dichloromethane) to yield the desired ester (0.51 g, yield 68%).

¹H NMR (CDCl₃): δ 1.5 (m, 4H), 1.7 (quintet, 2H), 1.8 (quintet, 2H), 1.9 (s, 3H), 4.1 (t, 2H), 4.2 (m, 2H), 5.6 (quintet, 1H), 6.2 (m, 1H), 6.4 (d, 1H), 7.4 (m, 3H), 7.6 (d, 2H), 7.7 (d, 1H), 8.2 (d, 2H). IR (KBr pellet, cm⁻¹): 2960, 1700, 1610, 1570,

1480, 1240, 1220, 1130, 1060, 720. MS (*m/e*): 450, 423, 381, 364, 340, 309, 289, 189, 133, 121, 93, 69.

Poly{6-[(4-((6-(Methacryloyloxy)hexyl)oxy)benzoyl)oxy]coumarin} (1). A solution of 6-[(4-((6-(methacryloyloxy)hexyl)oxy)benzoyl)oxy]coumarin (0.30 g, 0.0007 mol) and 1,1'-azobis(cyclohexanecarbonitrile) (0.0008 g, 0.0003 mmol) in *N,N*-dimethylformamide (5 cm³) was heated at 60 °C overnight. The cooled reaction solution was diluted with more *N,N*-dimethylformamide (10 cm³) and added dropwise with vigorous stirring to methanol (900 cm³). The resultant precipitate was filtered off, dissolved again in *N,N*-dimethylformamide (30 cm³) and reprecipitated from methanol (200 cm³). This procedure was repeated until no more monomer was present by TLC and a white solid was obtained (0.05 g, yield 16.7%).

7-[(4-((6-(Methacryloyloxy)hexyl)oxy)benzoyl)oxy]coumarin.¹⁶ A solution of *N,N*-dicyclohexylcarbodiimide (3.71 g, 0.018 mol) and dichloromethane (50 cm³) was added dropwise to a stirred solution of 4-((6-(methacryloyloxy)hexyl)oxy)benzoic acid (5.61 g, 0.018 mol), 7-hydroxycoumarin (2.92 g, 0.018 mol), and 4-(dimethylamino)pyridine (0.22 g, 0.0018 mol) in dichloromethane (50 cm³), and the reaction was stirred until completion (TLC). This reaction was stirred at room temperature overnight and then worked up and purified as described for 7-[(4-((6-(methacryloyloxy)hexyl)oxy)benzoyl)oxy]coumarin to yield the desired ester (5.55 g, yield 61.0%), with mp Cr-SmA 103 °C and SmA 106 °C (lit. mp 98–104.5 °C).¹⁶

¹H NMR (CDCl₃): δ 1.5 (m, 4H), 1.7 (quintet, 2H), 1.8 (quintet, 2H), 2.0 (s, 3H), 4.0 (t, 2H), 4.2 (t, 2H), 5.6 (quintet, 1H), 6.1 (quintet, 1H), 6.5 (d, 1H), 7.0 (d, 2H), 7.15 (d, 1H), 7.2 (d, 1H), 7.5 (d, 1H), 7.7 (d, 1H), 8.2 (d, 2H). IR (KBr pellet, cm⁻¹): 2940, 1740, 1710, 1610, 1510, 1320, 1250, 1230, 1170, 1050, 850, 760, 650. MS (*m/e*): 450, 398, 365, 340, 317, 289, 239, 203, 147, 133, 121, 104, 83, 76, 55, 41.

Poly{7-[(4-((6-(Methacryloyloxy)hexyl)oxy)benzoyl)oxy]coumarin} (2).¹⁶ A solution of 7-[(4-((6-(methacryloyloxy)hexyl)oxy)benzoyl)oxy]coumarin (2.55 g, 5.6 mmol) and 1,1'-azobis(cyclohexanecarbonitrile) (0.0075 g, 0.003 mmol) in *N,N*-dimethylformamide (12.5 cm³) was heated at 60 °C overnight. The reaction was worked up and the polymer purified as described for polymer 1 to yield the desired polymer 2 (2.20 g, yield 86.3%).

7-(Methacryloyloxy)coumarin.^{16,18} A solution of 7-hydroxycoumarin (3.24 g, 0.02 mol), 2-methacryloyl chloride (2.10 g, 0.02 mol), triethylamine (2.02 g, 0.02 mol), and dichloromethane (50 cm³) was stirred overnight at room temperature and then poured onto ice. The reaction mixture was worked up and purified as described for 4-((6-(methacryloyloxy)hexyl)oxy)benzoic acid to give the desired ester (3.55 g, yield 76.8%). Mp: 145–147 °C (lit. mp 146–147 °C).¹⁸

¹H NMR (CDCl₃): δ 2.0 (s, 3H), 5.9 (s, 1H), 6.3 (s, 1H), 6.5 (d, 1H), 7.2 (d, 1H), 7.3 (s, 1H), 7.8 (d, 1H), 8.1 (d, 1H). IR (KBr pellet, cm⁻¹): 3050, 2960, 1740, 1720, 1640, 1260, 1125, 960, 825. MS (*m/e*): 230 (M⁺), 162, 134, 105, 89, 77, 69, 58, 51.

Poly(7-(Methacryloyloxy)coumarin) (3).^{16,18} A solution of (1.00 g, 0.0043 mol), 1,1'-azobis(cyclohexanecarbonitrile) (0.052 g, 0.000215 mol), and *N,N*-dimethylformamide (10 cm³) was heated at 60 °C overnight. The reaction solution was worked up and purified as described for the polymer 1 to give the desired polymer 3 (0.67 g, yield 67%), mp 206 °C (lit. mp 200 °C).¹⁸

7-((6-Hydroxyhexyl)oxy)coumarin.¹⁸ A solution of 6-bromohexanol (3.62 g, 0.02 mol), 7-hydroxycoumarin (3.24 g, 0.02 mol), potassium carbonate (11.04 g, 0.08 mol), and butanone (50 cm³) was heated at 80 °C overnight. The cooled reaction solution was filtered to remove inorganic material and then evaporated down. The crude product was purified using column chromatography on silica gel (20% ethyl acetate in dichloromethane) to give the desired ether as an oil (4.70 g, yield 89.7%).

¹H NMR (CDCl₃): δ 1.2–2.0 (m, 8H), 3.70 (t, 2H), 4.0 (t, 2H), 6.2 (d, 1H), 6.8 (m, 2H), 7.4 (d, 1H), 7.6 (d, 1H). IR (KBr pellet, cm⁻¹): 3500, 2960, 1740, 1660, 1460, 1325, 1260, 1125, 825, 625. MS (*m/e*): 262 (M⁺), 162, 134, 105, 89, 63, 55.

(22) Harayame, T.; Katsuno, K.; Nishioka, H.; Fujii, M.; Nishita, Y.; Ishii, H.; Kaneko, Y. *Heterocycles* **1994**, *39*, 613.

7-((6-(Methacryloyloxy)hexyl)oxy)coumarin.¹⁸ A solution of methacryloyl chloride (1.05 g, 0.01 mol) and dichloromethane (20 cm³) was added dropwise to a solution of 7-((6-hydroxyhexyl)oxy)coumarin (2.62 g, 0.01 mol), triethylamine (1.01 g, 0.01 mol), and dichloromethane (20 cm³) at 0 °C. The reaction mixture was stirred until completion (TLC) and then poured onto ice. The organic layer was then separated off, washed with 10% hydrochloric acid (3 × 20 cm³) and 10% sodium hydroxide solution (3 × 20 cm³), and then dried (Mg₂-SO₄). The crude product was then purified using column chromatography on silica gel (20% ethyl acetate in dichloromethane) to give the desired ester as an oil (2.0 g, yield 44%).

¹H NMR (CDCl₃): δ 1.2–1.9 (m, 8H), 2.0 (s, 3H), 4.0 (t, 2H), 4.2 (t, 2H), 5.6 (s, 1H), 6.1 (s, 1H), 6.2 (d, 1H), 6.8 (m, 2H), 7.4 (d, 1H), 7.6 (d, 1H). IR (KBr pellet cm⁻¹): 2960, 1740, 1720, 1640, 1425, 1260, 1125, 825. MS (*m/e*): 330 (M⁺), 201, 175, 162, 134, 105, 83, 77, 69, 62, 55.

Poly[7-((6-(Methacryloyloxy)hexyl)oxy)coumarin] (4).¹⁸ A solution of 7-((6-(methacryloyloxy)hexyl)oxy)coumarin (1.20 g, 0.0036 mol), 1,1'-azobis(cyclohexanecarbonitrile) (0.04 g, 0.00018 mol) and *N,N*-dimethylformamide (10 cm³) was heated at 60 °C overnight. The reaction solution was worked up and purified as described for polymer **1** to give the desired polymer **4** (0.86 g, yield 72%), *T*_g 151 °C (lit. *T*_x 140 °C).¹⁸

7-((6-Bromohexanoyl)oxy)coumarin. A solution of 6-bromohexanoyl chloride (2.13 g, 0.01 mol), 7-hydroxycoumarin (1.62 g, 0.01 mol), triethylamine (1.01 g, 0.01 mol), and dichloromethane (25 cm³) was stirred at room temperature overnight and then poured onto ice. The organic layer was then separated off, washed with 10% hydrochloric acid (3 × 20 cm³), 10% sodium hydroxide solution (3 × 20 cm³), and then dried (Mg₂SO₄). The crude product was then purified using column chromatography on silica gel (10% ethyl acetate in dichloromethane) to give the desired ester (2.61 g, yield 77.0%).

¹H NMR (CDCl₃): δ 1.6–1.9 (m, 6H), 2.6 (t, 2H), 4.1 (t, 2H), 6.4 (d, 1H), 6.9 (m, 2H), 7.5 (d, 1H), 7.7 (d, 1H). IR (KBr pellet cm⁻¹): 3140, 2960, 1740, 1710, 1660, 1260, 1125, 860. MS (*m/e*): 340, 338 (M⁺), 204, 177, 162, 134, 77, 69.

7-((6-(Methacryloyloxy)hexanoyl)oxy)coumarin. A solution of methacrylic acid (0.26 g, 0.003 mol), 7-((6-bromohexanoyl)oxy)coumarin (1.0 g, 0.003 mol), and 2,3,4,6,7,8,9,10-octahydropyrimido[1,2-*a*]azepine (DBU) (0.46 g, 0.003 mol) in benzene (10 cm³) was heated under reflux overnight. The reaction mixture was then poured onto water. The organic layer was separated off, dried (MgSO₄), and filtered, and then the solvent was removed under reduced pressure to yield the desired ester (0.76 g, yield 73.4%), mp 108.5 °C.

¹H NMR (CDCl₃): δ 1.2–1.9 (m, 6H), 2.6 (s, 3H), 4.0 (t, 2H), 4.1 (t, 2H), 5.5 (s, 1H), 6.1 (s, 1H), 6.3 (d, 1H), 6.9 (m, 2H), 7.4 (d, 1H), 7.6 (d, 1H). IR (KBr pellet cm⁻¹): 3140, 2960, 1740, 1720, 1620, 1460, 1260, 1125, 860. MS (*m/e*): 344 (M⁺), 183, 162, 134, 115, 97, 77, 69, 55.

Poly[7-((6-(Methacryloyloxy)hexanoyl)oxy)coumarin] (5). A solution of 7-((6-(methacryloyloxy)hexanoyl)oxy)coumarin (1.00 g, 0.0029 mol), 1,1'-azobis(cyclohexanecarbonitrile) (0.036 g, 0.000145 mol), and *N,N*-dimethylformamide (10 cm³) was heated at 60 °C overnight. The reaction solution was worked up and purified as described for polymer **1** to give the desired polymer **5** (0.31 g, yield 31%).

Experimental Results

Previous results show that irradiation of the coumarin side-chain polymer **2** with polarized UV light gives homogeneous alignment with an azimuthal orientation dependent on incident fluence. This is illustrated in Figure 2, which shows Φ as a function of laser fluence. Symmetry would dictate that Φ is either parallel or perpendicular to the UV polarization direction, **P**, onto the alignment layer. Small deviations of Φ from 0 or 90° are found because of a finite azimuthal anchoring energy. The results show that the LC alignment direc-

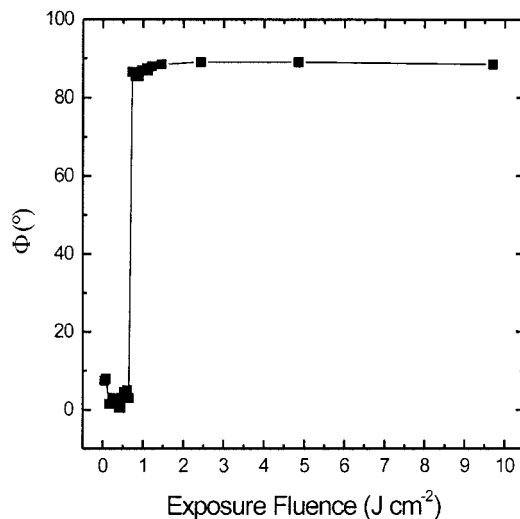


Figure 2. LC alignment direction at the photoaligned surface, measured with respect to **P** as a function of UV fluence incident on the alignment layer.

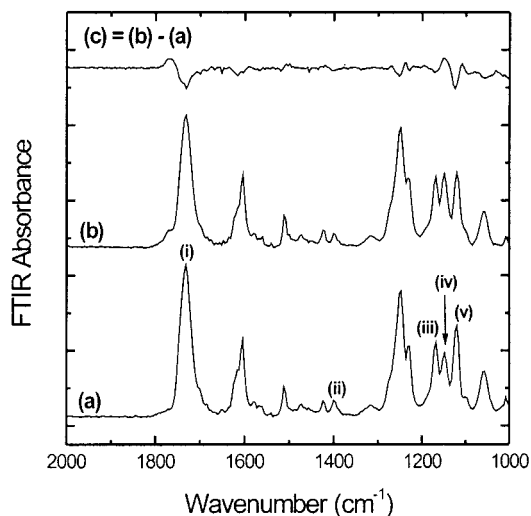


Figure 3. FTIR spectra of **2**: (a) before exposure; (b) after illumination at 300 nm with a fluence of 0.73 J cm⁻². The difference between the two spectra, (a) - (b), is shown in (c).

tion is parallel to the polarization direction of the incident UV light on exposure with low fluences. Then, at a critical fluence of 0.72 J cm⁻² a sharp transition to an orientation perpendicular to **P** is found. We now present spectroscopic data to elucidate the different origins of the parallel and perpendicular alignment.

FTIR Spectroscopy. Figure 3 a,b shows the FTIR spectrum of **2** prior to and after irradiation with UV light in air at 300 nm, respectively. The fluence used is 0.73 J cm⁻², which is close to the critical fluence for the LC alignment transition. The difference between the two spectra is shown in Figure 3c. Assignment of the various peaks to their corresponding vibrational modes is presented in Table 2.^{18,23} Both the unirradiated and irradiated samples show sharp IR transitions and the differences between them can mostly be attributed to the (2 + 2) cycloaddition process. The relevant bands are labeled i–v. On exposure of the sample, a new carbonyl peak (C=O) at 1768 cm⁻¹ joins the principal

(23) Li, W.; Lynch, V.; Thompson, H.; Fox, M. A. *J. Am. Chem. Soc.* **1997**, *119*, 7211.

Table 2. Assignment of the Various Peaks of the FTIR Spectra of **2 to their Corresponding Vibrational Modes prior to and after Irradiation with UV Light in Air at 300 nm**

peak wavenumber (cm ⁻¹)	assignt ^a
1768	C=O stretching (syn H-H dimer)
1732	C=O stretching
1603	ring C=C stretching
1512	ring C=C stretching
1472	CH ₂ scissor
1424	CH ₂ scissor
1401	<i>cis</i> C=C stretching
1248	predominantly C-C-O stretching (ester)
1230	=C-O-C asym stretching
1149	unconjugated ester stretching
1120	C(C=O)-O sym stretching
1057	=C-O-C sym stretching

^a The following abbreviations are used: sym, asymmetric; asym, for asymmetric.

carbonyl-stretching band (i) centered at 1732 cm⁻¹. This peak splitting is due to the formation of a nonconjugated carbonyl group in the cyclobutane photoproduct as a consequence of the cyclization reaction. The conjugated enone carbonyl group present in the coumarin ring of the unreacted starting material is converted into a nonconjugated carbonyl function due to the breaking of the C=C bond to form the cyclobutane ring on absorption of the UV light.^{17,18} According to Li et al.,²³ the peak is characteristic of the C=O stretching of the syn head-to-head (H-H) photodimer, whereas a peak at a lower wavenumber would indicate the existence of the syn head-to-tail (H-T) photodimer. Hence, we assume that the major dimerization product is the syn H-H regioisomer. The peaks iii-v, at 1248, 1150, and 1120 cm⁻¹, respectively, are all associated with ester stretching. Peaks iii and v show a splitting with an increase of intensity at lower wavenumbers on exposure, while the transition iv shows a large increase in intensity. These changes can all be attributed to the loss of enone conjugation in the coumarin by cycloaddition,^{17,18} but the assignments are tentative because of other ester stretching groups in the polymer. The most conclusive evidence for cross-linking is found from examination of the weak transition ii at 1401 cm⁻¹, originating from the stretching absorption of the *cis*-carbon-carbon double bond (C=C) in the enone function present in the coumarin side chain. Figure 4 shows that its peak intensity initially decreases rapidly with fluence and has dropped by 30% at the critical fluence for the LC alignment transition. The rate of C=C bond breaking by (2 + 2) cycloaddition to form the cyclobutane photoproduct saturates at higher fluences. These results show that the cycloaddition reaction requires only weak UV illumination in order to proceed efficiently and suggests that the cross-linking process induces the initial parallel LC alignment. The transitions i and iii-v similarly show large changes with fluence at low exposure, which further supports their association with cross-linking.

Figure 5a,b shows the FTIR spectrum of **2** prior to and after UV illumination in air using a fluence of 19.4 J cm⁻². The difference between the spectra is shown in Figure 5 c. The transitions from the exposed sample are broadened, and all show a significant decrease of peak intensity. The FTIR spectroscopy of photoaligning polyimide shows similar changes on exposure as a result of

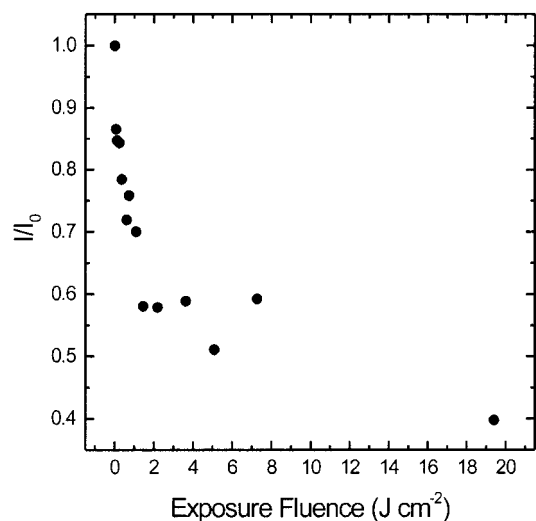


Figure 4. Normalized absorbance of the *cis* C=C stretching of the coumarin group as a function of fluence.

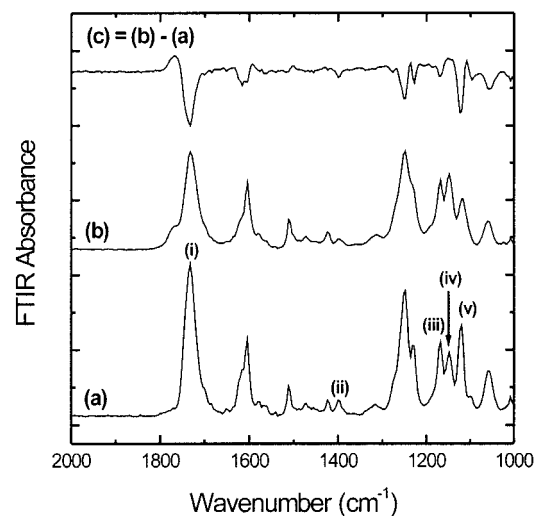


Figure 5. FTIR spectra of **1**: (a) before exposure; (b) after illumination at 300 nm with a fluence of 19 J cm⁻². The difference between the two spectra, (a) - (b), is shown in (c).

photodegradation.²⁴ This involves the breaking of photo-sensitive bonds causing a reduction of their characteristic absorption peaks. The spectral changes shown in Figure 5 are attributed primarily to photodegradation rather than additional cross-linking because the large decreases of peak intensity of transitions i, iii, and v are accompanied by much smaller increases of intensity at the wings, the latter being characteristic of cross-linking. A decrease in intensity occurs for both intact and cross-linked transitions. For example, Figure 6a shows the decrease of the normalized intensity of the transition at 1248 cm⁻¹, originating from C-O-C stretching bonds which are not involved in cycloaddition, as a function of incident fluence. The variation of intensity of the FTIR peak iv with UV fluence is shown in Figure 6b. The initial growth of this peak indicates cycloaddition, and its subsequent reduction is associated with photodegradation. Although it has been reported by others that photocleaving of dimerized photoproducts can be achieved by exposure to UV light in the 200-

(24) Lu, J.; Deshpande, S. V.; Gulari E.; Kanicki, J.; Warren, W. L. *J. Appl. Phys.* **1996**, *80*, 5028.

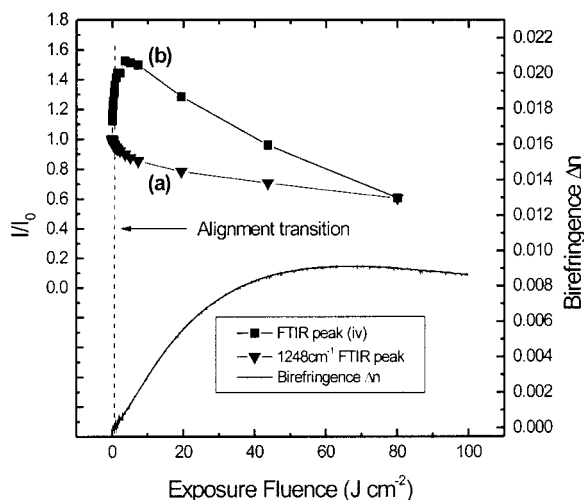


Figure 6. Variation in the absorbance of FTIR peaks: (a) at 1248 cm^{-1} ; (b) peak iv with incident UV fluence; (c) variation of the birefringence of **2** with incident UV fluence.

350 nm wavelength range,^{17,25,26} there is no direct evidence for the cleavage of dimers from the FTIR results discussed here. Photocleavage would lead to the recovery of transition ii, and Figure 4 shows that this does not occur. A standard signature of oxidative photochemical degradation is the appearance of a very broad band between 3700 and 2500 cm^{-1} , which is assigned to the stretching mode of hydroxy (O–H) groups.^{27,28} Hydrogen bonding between the carboxylic acids gives rise to the formation of loosely bonded dimers of carboxy groups with broad absorption bands. This indicates a subsequent reaction of free radicals, formed on absorption of high-intensity UV radiation, with molecular oxygen present in the atmosphere above the polymer layer to form a carboxylic acid function. The FTIR spectra of analogous samples exposed in a nitrogen (N_2) atmosphere show similar decreases in absorption peaks, but as expected, no evidence of additional absorption attributable to carboxyl or hydroxy functions of new carboxylic acid groups.

Birefringence. Figure 6c shows the variation with incident UV fluence of the film birefringence, Δn , at 633 nm recorded during polarized UV illumination. The birefringence increases with fluence from zero and has a negative sign; i.e., the easy axis of the polymer is perpendicular to **P**. The resonant energy of the dimer is greater than that of the unreacted side chains because of the loss of conjugation on formation of the latter. Hence, the birefringence is associated with the anisotropy of intact polymer side chains still incorporating the conjugated enone function rather than dimerized side chains in the cross-linked network. The latter incorporates an aliphatic cyclobutane group in place of the two conjugated carbon–carbon double bonds present in the former. As discussed above, the initial growth of peak iv, shown in Figure 6b, indicates cycloaddition and

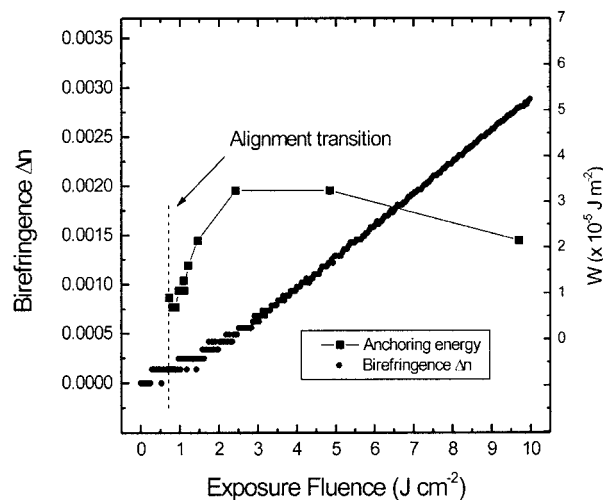


Figure 7. Birefringence of **2** shown as a function of fluence up to 10 J cm^{-2} . The dashed vertical line indicates the critical fluence for the transition from parallel to perpendicular alignment. The azimuthal anchoring energy is also shown as a function of fluence above the critical fluence.

its subsequent reduction is associated with photodegradation. The generation of Δn is independent of cycloaddition, since it reaches a maximum at a fluence of 65 J cm^{-2} long after cycloaddition has ceased. Instead, Δn originates from the selective photodegradation of both dimerized and unreacted side chains oriented parallel to **P**. Although photodegradation continues with higher fluences, the birefringence decreases because of the isotropy of the photodegraded products.

Discussion

The results so far show that UV illumination of side-chain polymers containing coumarin induces two distinct photochemical processes with a quite different dependence on fluence. Cross-linking by $(2 + 2)$ cycloaddition occurs at very low fluences and saturates when about 40% of the side chains have been dimerized; see Figure 4. Photodegradation of both unreacted and cross-linked side chains occurs more slowly, and the birefringence of the material is dependent upon anisotropic photodegradation of the intact side chains. We now relate these spectroscopic observations to different mechanisms giving homogeneous LC photoalignment parallel and perpendicular to **P**.

Origin of Parallel Alignment. Figure 7 shows the Δn as a function of fluence up to 10 J cm^{-2} . The dashed vertical line indicates the critical fluence for the transition from parallel to perpendicular homogeneous alignment with respect to **P**. The azimuthal anchoring energy is also shown as a function of fluence above the threshold. In the parallel alignment regime, Δn is extremely low, despite strong azimuthal anchoring—energies of about $2 \times 10^{-5}\text{ J m}^{-2}$ are obtained. The birefringence measurement was taken during UV illumination, and for these low fluences only, its value is further decreased by relaxation when the UV beam is removed. Cross-linking proceeds rapidly at these fluences, with the reaction probability of the first step given by $\mathbf{P} \cdot \mathbf{m} = Pm \cos^2 \varphi$, where φ is the azimuthal angle between **P** and **m**, the polarization vector of the side chain. Hence an anisotropic distribution with

(25) Chen, Y.; Hong, R.-T. *J. Polym. Sci., Part A: Polym. Chem.* **1997**, *35*, 2999.

(26) Chang, J. S.; Kim, H. S. *Korea Polym. J.* **1995**, *3*, 12.

(27) Culthrop, N. B.; Daly, L. H.; Wiberley, S. E. *Introduction to Infra Red and Raman Spectroscopy*, 2nd ed.; Academic Press: New York, 1975.

(28) Silverstein, R. M.; Bassler, G. C. *Spectroscopic Identification of Organic Compounds*, 2nd ed.; Wiley: New York, 1967.

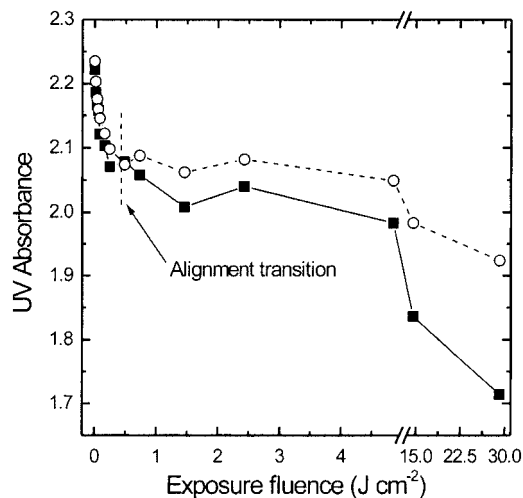


Figure 8. Peak absorbance of exposed **1** as function of polarized fluence at 300 nm. The probe beam at 264 nm is polarized parallel (■) and perpendicular (○) to **P**.

maximum side-chain density perpendicular to **P** is expected. Instead, the negligible Δn at low fluences implies that the distribution of the polymer side chains incorporating unreacted coumarin is isotropic. Independent verification of side-chain isotropy in the parallel alignment regime is provided by Figure 8 which shows the peak absorbance of **1** as a function of incident fluence for probe polarization parallel and perpendicular to **P**. There is negligible dichroism for low-incident fluences despite high reactivity. The low birefringence and its relaxation can be explained by assuming that the unreacted side chains are mobile in the early stages (up to 30%) of cross-linking. Parallel alignment must then originate from the photoproducts. Dimerization occurs selectively for the side chains whose transition moments are parallel to **P**, so that an anisotropic distribution of dimerized cyclobutane side chains is expected with maximum density parallel to **P**. Molecular modeling⁸ and dichroic FTIR¹⁹ confirm this result. We believe that this anisotropy is maintained despite the mobility of the unreacted side chains because of the steric hindrance of the cross-linked dimer to movement. The negligible birefringence suggests that dispersive interactions do not determine surface LC-alignment in the parallel alignment regime. We believe that the alignment involves a steric interaction between LC molecules and the cross-linked syn H–H photoproduct.

Origin of Perpendicular Alignment. The birefringence and azimuthal anchoring energy increase with fluence above the critical fluence for the change in LC-alignment direction from parallel to perpendicular. Both photodegradation and cross-linking have anisotropic photochemical reaction probabilities proportional to $\cos^2 \varphi$, which results in the maximum density of intact side chains perpendicular to **P**. The anisotropy of the unreacted side chains is maintained in the perpendicular alignment regime, because of the increased viscosity resulting from a high cross-linked density. The associated rise of both birefringence and anchoring strength before saturation, as shown in Figure 7, confirms previous suggestions that perpendicular LC alignment originates from the anisotropic distribution of intact side chains. It also suggests that a dispersive LC–surface interaction now determines LC alignment. This work

shows that photodegradation provides the major source of the anisotropy. Photodegradation involves the breaking of photosensitive bonds so that the LC dispersive interaction is reduced parallel to **P**. Hence the LC alignment direction corresponds to that of the maximum density of intact side chains. Polarized UV absorbance to be published elsewhere show that the photoproducts have an isotropic distribution and so cannot contribute to the azimuthal alignment. Once the side chains become immobile, cross-linking could also contribute to the anisotropy at low fluences since the dispersive LC interaction with photodimers (aligned parallel to **P**) is smaller than that with intact side chains. However Figure 4 shows that most of the cross-linking occurs before the critical fluence so we believe that the contribution of cross-linking to the perpendicular alignment is small. Indirect confirmation of the importance of anisotropic photodegradation in determining LC photoalignment is found by measuring the anchoring strength of a photoalignment layer, which was illuminated with UV light, rinsed with an organic solvent in order to remove any residual unreacted material and/or soluble photodegradation products, and subsequently dried. The azimuthal anchoring energy increased because of the removal of photodegradation products. These are shown by polarized UV and FTIR spectra to have a primarily isotropic distribution.

Implications of Photodegradation. It is well-known that polarized UV illumination of polyimide provides an anisotropic photodegradation resulting in LC alignment perpendicular to **P**,^{4,29,30} the direction with maximum density of intact polymer chains. Photodegradation products are thought to impair the optical performance of an LCD incorporating a UV-irradiated polyimide photoalignment layer. The polar anchoring energy of photoaligned polyimide is found to be 10 times lower than that of rubbed polyimide possibly because of the lowering of the surface energy caused by decomposition.³⁰ The electrical performance of the display can also be compromised in a similar fashion. Capacitance–voltage experiments show that a net negative charge is created in the photoaligned film.²⁴ This may result from carboxylic acid formation³¹ and gives rise to image sticking and display flicker. The thermal stability of polyimide photoaligned at room temperature is poor, because of subsequent relaxation of the residual polymer segments on annealing. Despite these potential problems, the impact of photodegradation on the performance of LCDs containing a photoalignment layer produced by a photochemical cross-linking reaction has not yet been considered in any detail. Photodegradation may be particularly important for materials where the cross-linking reaction is slow. For example, using the same photoalignment conditions as discussed here, about 8 J cm⁻² is required to achieve a saturated azimuthal anchoring energy for PVCi.¹⁰ It is likely that photodegradation rather than cross-linking or cis/trans isomerization is the primary photoalignment mechanism.

(29) Newsome, C. J.; O'Neill, M.; Bryan-Brown, G. P. *Proc. SPIE* **1999**, *3618*, 132.

(30) Hasegawa, M. *Jpn. J. Appl. Phys.* **1999**, *38*, L457.

(31) Yang K. H.; Tajima K.; Takenaka A.; Takano H. *Jpn. J. Appl. Phys.* **1996**, *35*, L561.

Generality of Results. We now compare our results to those reported by others in the field. Table 1 summarizes the quoted LC alignment direction for typical coumarin containing side-chain polymers **1–6**. It is clear that the development of parallel and/or perpendicular alignment depends on the specific composition of the polymer. For example, parallel alignment is retained for side chains with alkoxy units attached directly to the coumarin. This variation is consistent with our proposal that the development of parallel or perpendicular alignment depends on the competition between short-range LC steric interactions with cyclobutane photodimers and anisotropic LC dispersive interactions with intact coumarin side chains. The ensuing LC alignment direction depends on the differences between the photodimerization and photodegradation rates as well as the anisotropy of the latter. It is clear from the FTIR spectra presented by other authors^{16,19} that photodegradation is apparent even when parallel alignment is retained at higher fluences, although it is seldom referred to. This implies that the photodegradation of these materials is more isotropic: the flexibility of the intact side chains is maintained for higher fluences or the dispersive interaction is smaller. Standard commercial LCDs normally require strong LC anchoring with long-term stability. Although other workers report device instability after a couple of months because of swelling of the alignment layer,²⁰ our test cells show no deterioration in performance two years after fabrication. Cross-linked coumarins can achieve high azimuthal anchoring energies; thin layers of **2** cross-linked with polarized UV light show resolution limited values $>6 \times 10^{-5} \text{ J m}^{-2}$ when in the parallel alignment regime.¹⁰ Maximizing the cross-linked density by a postexposure with isotropic UV light should enhance the stability. Preliminary experiments show no deterioration in the anchoring strength of the alignment layer. Schadt and Seiberle report a similar result.¹⁷ A key parameter in the design of cross-linkable photoalignment materials is to achieve

a cross-linking rate much greater than that of photodegradation. This has been obtained for polymer **2** discussed in detail here. The use of derivatives of 6-hydroxy coumarin, such as polymer **1**, can further enhance the cross-linking rate.

Conclusion

Model side-chain polymers containing coumarin in the side chain have been shown to induce homogeneous LC alignment parallel and perpendicular to **P** for weak and strong polarized UV illumination, respectively. Spectroscopic analysis shows that the competition between two independent LC-surface interactions determines the resultant director orientation. For weak exposure, the coumarin in the polymer side chain is depleted rapidly by an anisotropic cross-linking reaction, but intact side chains retain a residual isotropic distribution because of their in-plane mobility. We suggest that the LC alignment direction is determined by a steric interaction with the dimerized cyclobutane side chains, which maintain anisotropy due to their rigidity. The subsequent increase in the anisotropy of the intact side chains is predominantly the result of photodegradation and is accompanied by a switch in the LC alignment direction from parallel to perpendicular above a critical fluence. We believe that a dispersive LC interaction with intact side chains gives perpendicular alignment. Photodegradation may also be the cause of the perpendicular LC photoalignment obtained using many other cross-linkable polymers.

Acknowledgment. We wish to thank the EPSRC for provision of an Advanced Fellowship (S.M.K.), postdoctoral Fellowships (P.H. and W.L.D.) and postgraduate studentships (P.O.J. and G.J.O.). DERA, Malvern, U.K., are thanked for further financial support.

CM0011413